Second Attempt to Break 10 kWh/kg Energy Consumption Barrier Using a Wide Cell Design

Marc Dupuis
Consultant, GeniSim Inc, Jonquière, Québec, Canada
Corresponding author: marc.dupuis@genisim.com

Abstract

In this year's ALUMINIUM article [1], the author selected a wide cell design for breaking the 10 kWh/kg cell specific energy consumption barrier. In the study presented in that article, the lowest value of 10.2 kWh/kg Al was obtained. Yet, in that study, the reduction of the metal pad thickness left plenty of spare cell cavity. This provides space to increase the thickness of the cell lining below the cathode block. There is also the opportunity to use new semi-insulating lining materials that resist sodium penetration into the cell lining. This combination represents an opportunity to design a more insulating cathode lining and hence to reduce the cathode heat loss and the total cell heat loss. That same study also assumed that the lowest anode-to-cathode distance (ACD) was 2.8 cm, the lowest metal pad thickness was 10 cm, and the lowest cell superheat was 5 °C. Since then, operation below 2.5 cm of ACD has been reported so the current study will use 2.5 cm as lowest ACD, keeping the other two lowest limits unchanged. This design strategy can break the 10 kWh/kg Al energy consumption.

Keywords: Low energy consumption in aluminium electrolysis cells, wide cell design, cell heat balance, mathematical modeling of aluminium electrolysis cells.

1. Introduction

The work presented in this paper is part of a continuing effort to design a cell operating at the lowest possible energy consumption. The current goal is to break the 10 kWh/kg barrier starting with a design operating at 10.2 kWh/kg Al. In order to get to this already extremely low level of energy consumption, several important design changes or design innovations have already been implemented. Before proceeding with the presentation of the new work, the design change steps that led to the starting point of the current work are recapitulated here first.

1.1. Wide Cell Design

The first and very significant design change, compared to most recent high amperage cell designs, is the decision to go for a wide cell design that permits to place four anode carbon blocks through the width of the cell cavity. This in turn introduces two new longitudinal channels in addition to the usual center channel. As discussed in [2], the aim of adding those 2 extra longitudinal channels is to increase the bath volume and to decrease inhomogeneities present in the bath chemistry.

That cell design change innovation was promoted to the author by Barry Welch and was first presented in [2]. As already described in that ALUMINIUM article, using a wider cell permits the reduction of the ratio of external surfaces losing heat to the environment to the electrolysis surfaces. Another way to express this is to directly quote [2]: the usage of a wider cell is "*reducing the heat loss per unit production*", which is desirable if not required to minimize the cell energy consumption. Figure 1 is presenting the sketch of the very first wide cell design as presented in [2], and a more recent version presented in [3] produced by HHCellVolt, a software created by Peter Entner available in the Microsoft store [4].

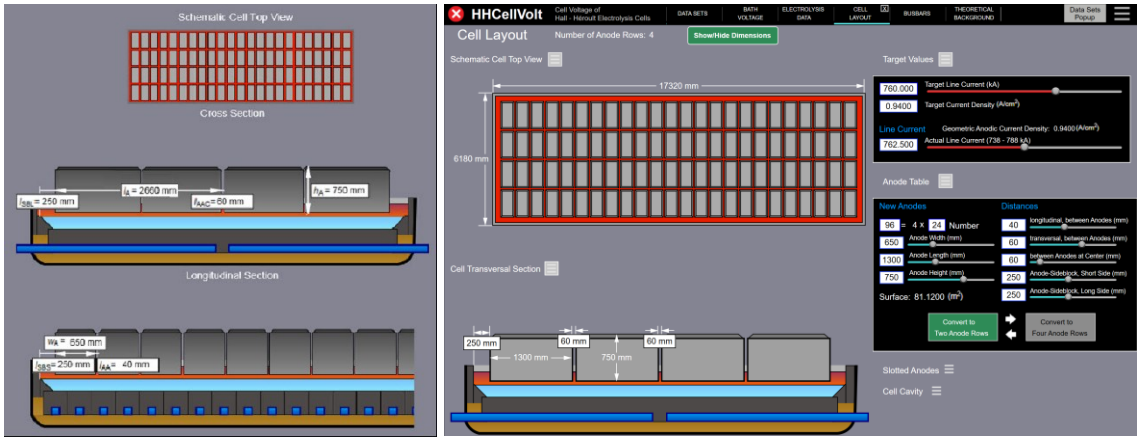

Figure 1. Sketch of the first wide cell design as presented in [2] on the left and a more recent version produced by HHCellVolt [4] as presented in [3] on the right.

1.2. Usage of Copper or Mostly Copper Collector Bars

As already described in [2], it would not have been possible to design a cell wide enough to place four regular size anode blocks through its width without the use of copper or mostly copper collector bars. Without it, it would not be possible to avoid the generation of very harmful horizontal current in the metal pad. Such a mostly copper collector bar design was first presented in [5] as a mean to mostly eliminate horizontal current in the metal pad and significantly reduce the cathode lining voltage drop. Figure 2 shows the mostly copper collector bar design used in [5]. It is essentially a copper conductor inserted in a thin steel tube that is cast iron rodded as usually done for steel collector bar. For a standard width cell design, using such a mostly copper collector bar design virtually eliminated the presence of horizontal current in the metal pad as illustrated in the calculated current density also presented in Figure 2.

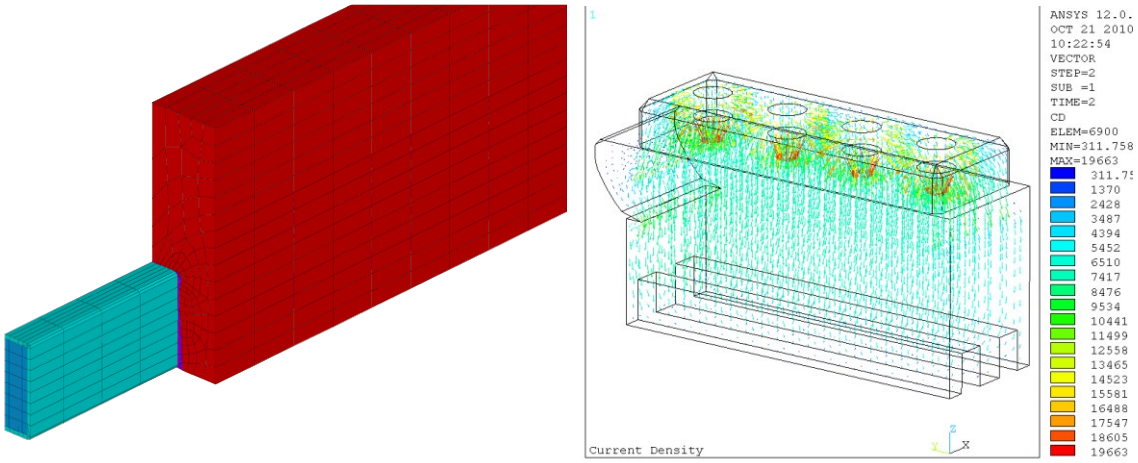

Figure 2. Mostly copper collector bar design on the left and resulting current density field on the right as presented in [5].

1.3. Design Feature that Reduces the Stubs and Collector Bar Heat Loss

As discussed in [6], it would not have been possible to use a mostly copper collector bar design without doing something to prevent those bars to dissipate an excessive amount of heat out of the cell. To avoid such a problem, a special design feature has been used in the design presented in [5]

without revealing it. That special design feature has been revealed in [6]. It is a simple local restriction of the conductor section that concentrates the current increasing the local Joule heat generation preventing an excessive amount of heat to pass through that local restriction. Figure 4 shows such a stub with local restriction, presented in [6]. In an extreme case, close to a fuse situation, the temperature will reach a maximum in that restricted section creating an adiabatic plane at that location preventing any heat flux to pass through. The current design is still quite far from that extreme situation as illustrated in Figure 3.

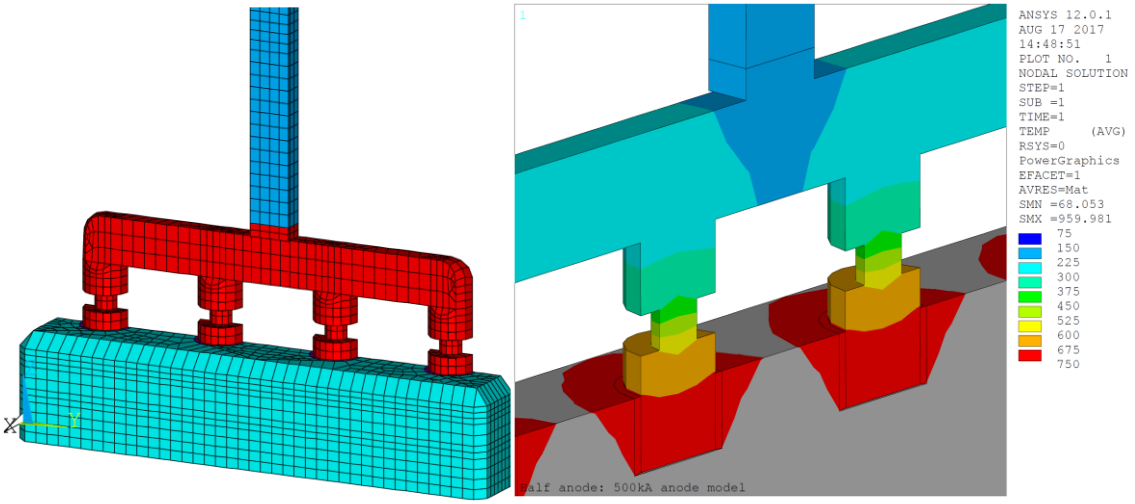

Figure 3. Local stub cross-section restriction as presented in [6].

1.4. Special Stub Hole Design Reducing the Stub to Carbon Voltage Drop

In order to produce a very low energy consumption cell design, the internal heat generation and the corresponding cell heat loss must be reduced by more than a half from a typical cell operation at approximately 13 kWh/kg Al. On the heat generation side, that means reducing the ohmic voltage drop of all the conductors: anode, cathode and busbar. On the anode side, the usage of big stub diameter connecting to a small square cross-section of carbon, as illustrated in Figure 3, permits a significant reduction of the anode voltage drop. In addition, a special stub hole design feature has been used since the design presented in [5] to further reduce the anode voltage drop by reducing the stub to carbon voltage drop. That special stub hole design feature has been revealed in [7]. It relies on a lock mechanism that prevents free vertical thermal expansion of the stub in the hole. Once constrained, that thermal expansion creates a strong contact pressure between the bottom face of the stub and the bottom of the carbon hole. With that strong contact pressure, the current can travel straight down from the stub to the carbon greatly reducing the stub to carbon voltage drop. Figure 4 illustrates the design and presents the resulting current path from the stub to the carbon block obtained by a thermo-electro-mechanical model.

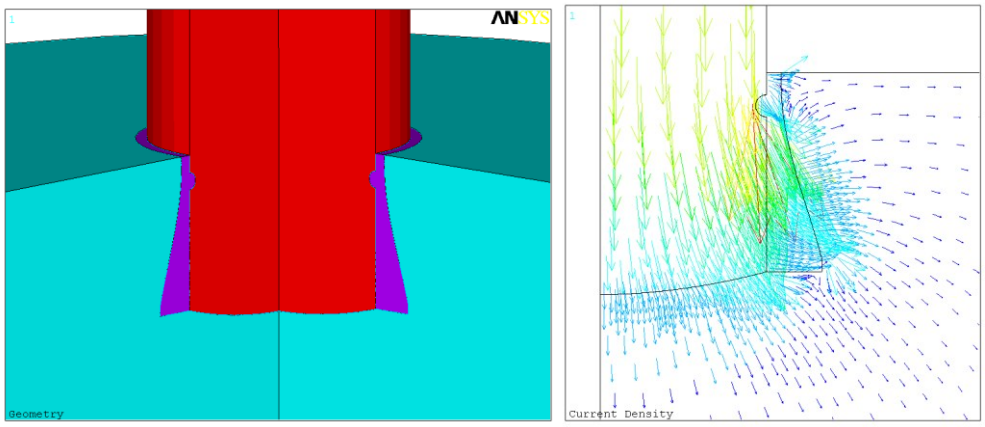

Figure 5. Special stub hole design as presented in [7].

1.5. Special "Spider" Yoke Assembly Design with 12 Stubs and Copper Insert

As presented in [8], in order to further reduce the anode voltage drop, a special "spider" yoke assembly has been designed. A copper insert is added to the very long yoke helping to reduce the voltage drop without increasing the anode heat loss. That yoke is located fairly high above the carbon block top surface in order to accommodate a very thick anode cover of 25 cm in the case reported in [8].

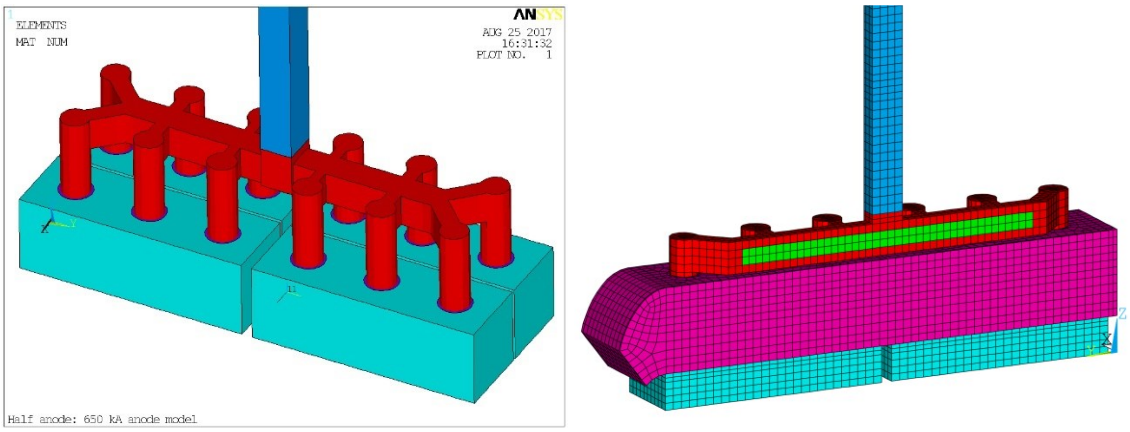

Figure 6. Special "spider" yoke assembly design as presented in [8], full anode sketch on the left and half anode finite element (FE) model mesh on the right showing the copper insert in green.

1.6. Extra Insulation in the Cathode Lining Pier Region

In order to be operated at the minimum possible cell energy consumption, the cell must be operated at the minimum possible bath superheat in order to minimize the cathode side wall heat loss. This in turn means that the lining design in the pier region must provide high insulation in order to avoid the ledge toe to grow excessively on the cathode surface. Figure 7 compares the standard pier height made of semi-insulating brick with an extended pier height design as presented in [9]. That extended pier height design is riskier to operate as it is increasing the chance of side wall tap out if the cell is operated at a very high bath superheat for an extended period of time. Clearly, a cell designed to be operated at the minimum possible cell energy consumption will be more sensitive to operational perturbations than a standard cell.

1.7. RCC Busbar Design with Alternating Upstream and Downstream Risers

There is no direct relationship between the width of the cell or potshell and the type of busbar design that can be selected. As described in [10], there is now 4 types of busbar design available: the classic Internal Compensation Current (ICC) busbar design that can be symmetric or asymmetric. The External Compensation Current (ECC) busbar patented by Pechiney in 1987 [11], the Combined Compensation Current (CCC) patented by Hydro Aluminium in 2011 [12], and the quite recent Reversed Compensation Current (RCC) described in [13].

As described in [2], the RCC busbar design with alternating upstream and downstream risers was selected to be used for the initial wide cell design as an efficient design to be able to minimize the pot to pot distance and the busbar voltage drop while ensuring a stable cell operation even at the minimum possible ACD. The most recent version of that RCC busbar for the wide cell is presented in [1] altogether with some results of the MHD cell stability analysis results for an operation with only 10 cm of metal pad thickness, selected to minimize the cathode heat loss.

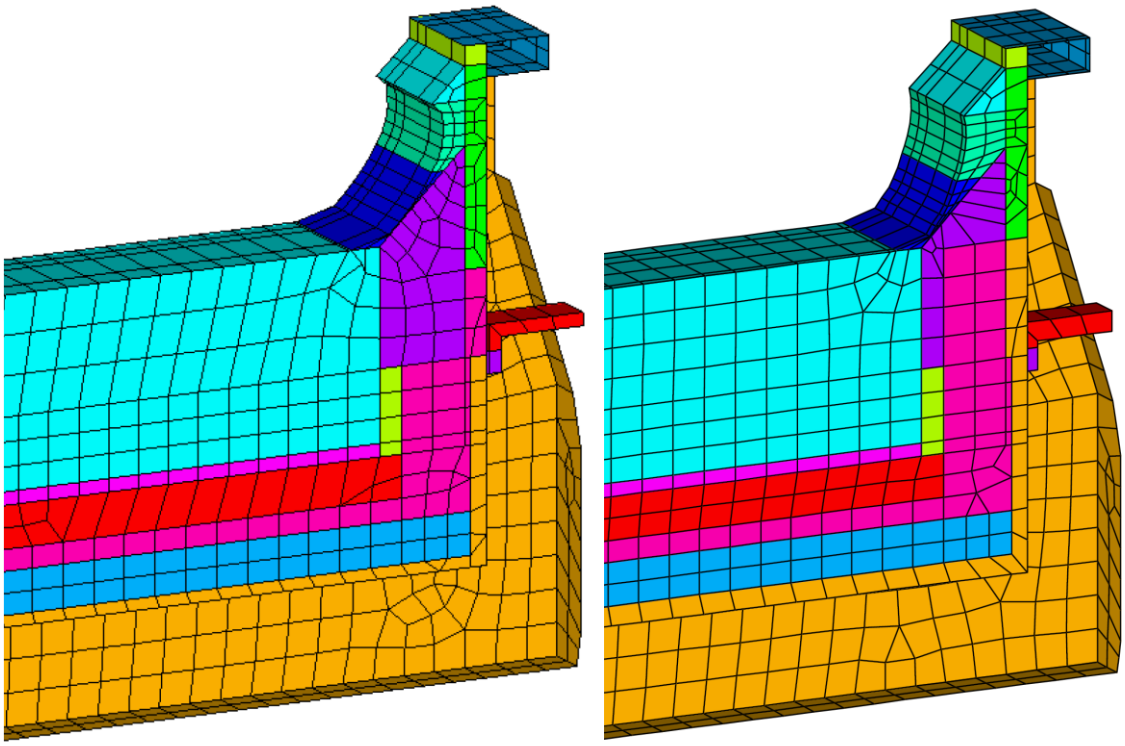

Figure 7. Comparison between a standard height pier design on the left and the extended height pier design on the right as presented in [9].

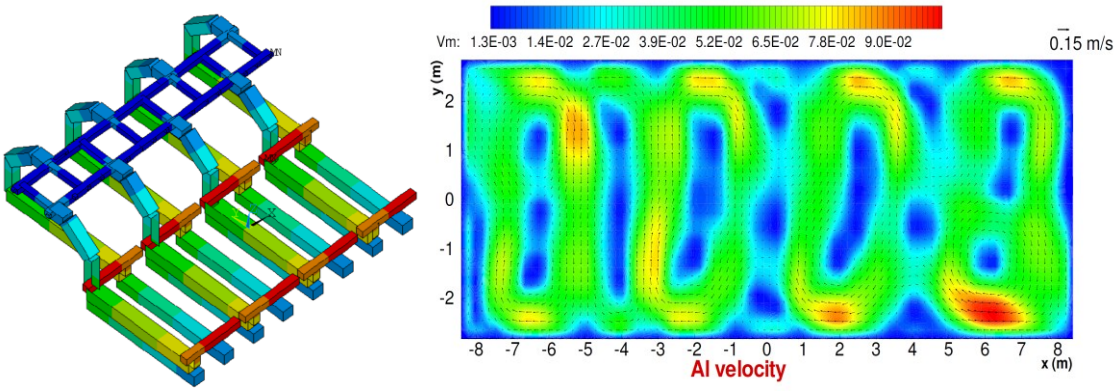

Figure 8. RCC busbar design with alternating upstream/downstream risers and corresponding metal flow solution as presented in [1].

1.8. Base Case, Wide Cell Design at 530 kA

The base case or starting point of the current work is the result of the implementation of all the above described design features in a wide cell operating at 530 kA as described in [1]. The key operating conditions are calculated using Dyna/Marc, a cell simulator developed by the author [14]. Those key results are presented in Table 1 on the left side. The ACD was selected to be 2.8 cm and the anode current density is only 0.66 A/cm^2 at 530 kA. In addition, the ohmic resistance of the cell conductors, anode, cathode and external is also extremely low, the total voltage drop of all those conductor together is only 502 mV. As a result, the total cell voltage is only 3.24 V. The current efficiency is predicted to be 94.3 %. Using the Haupin's equation to computes the equivalent voltage to make metal, cell internal heat is calculated to be only 516 kW for the cell operation at 10.2 kWh/kg Al. The predicted bath superheat is 5.0 °C which was assumed to be the minimum acceptable value. As explained in [1], it is that limit that prevented to reach the 10.0 kWh/kg Al target in the previous study.

2. Second Attempt to Break the 10 kWh/kg Al Barrier

As discuss in the future work section of [1], further reducing the cell energy consumption means at the same time reducing the cell voltage and the cell heat loss while still respecting the self-imposed design criteria like the minimum acceptable ACD and bath superheat.

2.1. Relaxing the Minimum ACD Limit to 2.5 cm

On the side of the self-imposed ACD limit, the selected value of 2.8 cm is based on that value being reported in Table 4 of [15] for the operation of the DX+ at 440 kA. Yet, very recently an operation at 2.3 cm ACD was reported in Figure 14 of [16] for the operation of the D18+ at 240 kA. In that same Figure 14, operation around 2.5 cm ACD is reported when the cells are operated between 220 and 235 kA. Based on those reported operational results, the author decided to relax its minimum ACD limit from 2.8 cm to 2.5 cm.

2.2. Replacing the Fire Brick by a New More Insulating yet Sodium Resistant Material

The reduction of the ACD will reduce the cell internal heat. If nothing else is changed, that in turn will lead to a reduction of the bath superheat. But the superheat had already reached its minimum allowed value of 5.0 °C, so other changes are required to prevent that to happen.

As mention in [1] future work section, new semi-insulating lining materials that resist sodium have recently become available. One such material is marketed by Skamol under the name Skamobar LE [17]. As Figure 9 illustrates, that new material resists very well a 48 hours sodium vapor test.

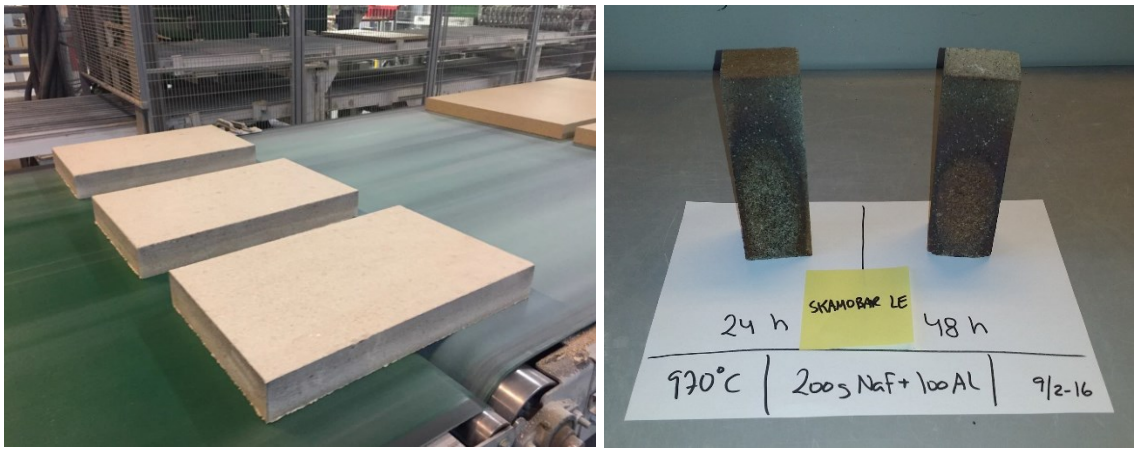

Figure 9. Skamobar LE manufacturing process and sodium vapor test results as presented in [17].

Since that new material resists sodium almost as well as a fire brick, the lining design was changed replacing the two fire brick layers under the cathode block by that semi-insulating Skamobar LE material. That change alone increased the thermal insulation of the cathode lining. In addition, as also discuss in the future work section of [1], reducing the metal pad thickness from 20 cm to 10 cm is offering the option to increase the global cathode lining thickness.
This has been done in the present work by adding an extra layer thickness of that new sodium resistant semi-insulating material. Figure 10 is presenting the obtained vertical temperature gradient in the lining below that cathode and the resulting heat flux.

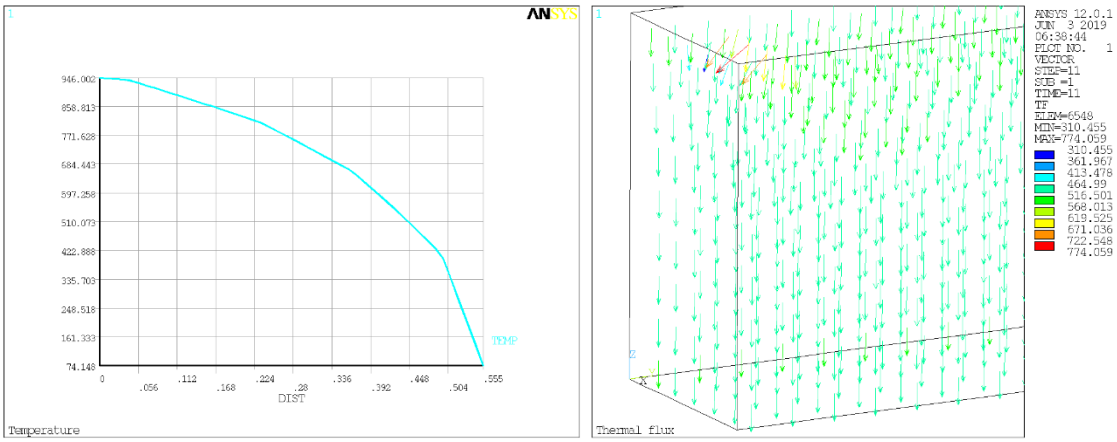

Figure 10. Vertical temperature gradient under the center of the cathode from the cathode bottom to the potshell and resulting vertical heat flux.

2.3. Introduction of a New Irregular Cathode Surface Design Feature

Irregular cathode surface designs have been studied and tested in the past as a way to increase the cell stability [18]. The cathode surface can also be machined at an angle in order to reduce the horizontal current in the metal pad [19].

In the current work, it is proposed to produce a cathode block that is 5 cm higher close to the edge of the block in order to contain the first 5 cm of the metal pad. This way, only the top 5 cm of the total 10 cm metal pad thickness is facing the side ledge and hence is dissipating heat out through the side wall. Figure 11 is showing a zoom of the ledge region of the model mesh and the resulting temperature solution with the converged ledge profile. That irregular cathode surface design is increasing a little the metal to cathode carbon surface area, so the cathode block must be very well insulated for that new design feature to actually reduce the cathode heat loss.

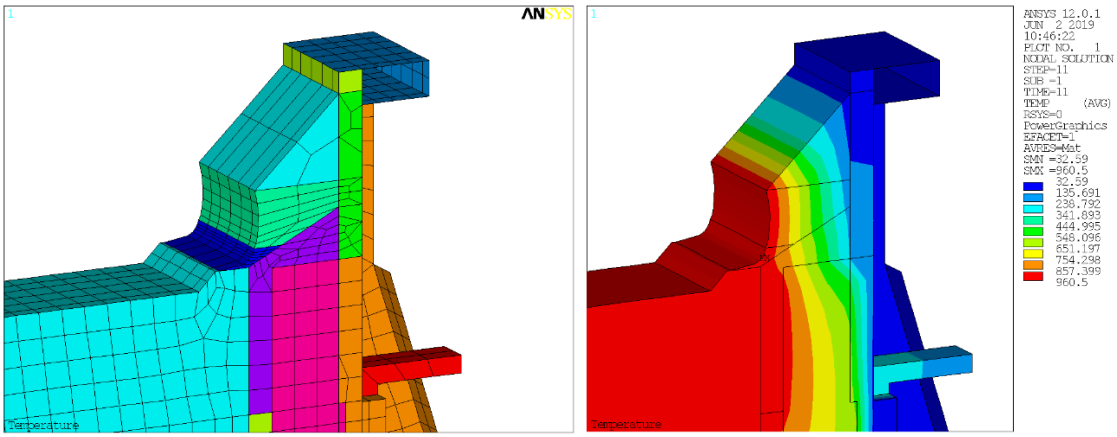

Figure 11. New irregular cathode surface design feature and corresponding temperature solution.

2.4. 3D ANSYS-Based Cathode Side Slice Thermo-Electric Model Results at 530 kA

The global lining design is presented on the left side of Figure 12, The cathode lining below the cathode block is now 65 mm thicker or 550 mm thick in total with 40 mm of bedding material, 195 mm of Skamobar LE sodium resistant semi-insulating material, 130 mm of standard semi-insulating brick, 130 mm of insulating brick and finally 60 mm of calcium silicate material. The edge of the cathode block is now 50 mm higher but the bulk of the cathode block is still 580 mm thick. The metal pad is still 10 cm thick but only the top 5 cm is facing the side ledge, the bottom 5 cm is contained by the cathode block. The right side of the Figure 12 is presenting a zoom of the temperature solution showing the very small section of the copper collector bar going out of the potshell.

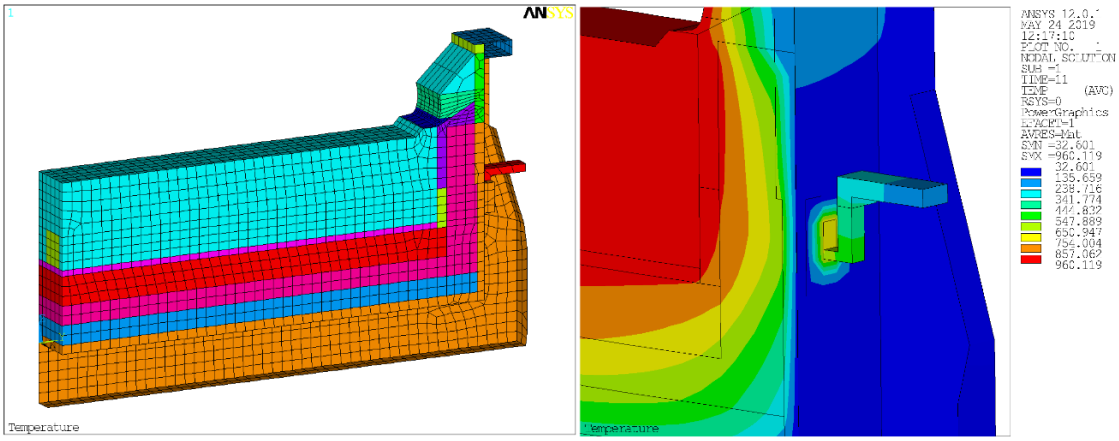

Figure 12. Global cathode side slice model mesh and resulting temperature solution near the collector bar exit zone.

The 3D ANSYS model is predicting an internal cathode drop of 102 mV and an external cathode drop of 44 mV. This is an increase of 12 mV as compared to the results presented in [1] produced by the increase of temperature in the cathode block and collector bar. The heat loss of the internal part of the cathode has been decreased to only 273 kW when the bath superheat is about 5 °C. This is a 38 kW or 12 % reduction as compared to the 311 kW obtained previously [1].

2.5. Dyna/Marc Global Analysis Results at 530 kA

As the right side of Table 1 indicates, reducing the ACD from 2.8 cm to 2.5 cm was sufficient to decrease the cell internal heat enough to bring the cell energy consumption exactly to 10.00 kWh/kg Al. On the cell heat loss side, despite that reduction of cell internal heat, the increase of the cell lining insulation more than compensated and as a result, the predicted bath superheat has increase to 5.8 °C. This means that there is a potential to further reduce the cell internal heat in order to decrease the cell energy consumption below 10 kWh/kg Al. Table 2 summarizes all the results obtained starting by the very first wide cell design operating at 762.5 kA and 12.85 kWh/kg Al, all sharing the same potshell platform. In order to go from that initial design operating at 0.93 A/cm^2 of anode current density and dissipating 1328 kW to an operation at 10 kWh/kg, the anodic current density had to be reduced by 29 % to 0.66 A/cm^2 and the heat loss had to be reduced to 478 kW which is only 36 % of what it was initially.

Because the author is only working very sporadically on this demonstration cell retrofit work, Table 2 is summarizing results gradually published over several years, highlighting the step by step nature of the cell retrofit work. In a real retrofit project, this would have been done in the framework of the cell development cycle with the construction and operation of prototypes of most if not all steps so the elapsed time would have been even greater.

Table 1. Dyna/Marc steady-state solution summary at 530 kA, left 2.8, right 2.5 cm ACD.

Steady State Solution

Cell amperage	530.0 [kA]
Anode to cathode distance	2.80000 [cm]
Operating temperature	961.560 [C]
Ledge thickness, bath level	15.79983 [cm]
Ledge thickness, metal level	9.99283 [cm]
Bath chemistry:	
Cryolite ratio	2.20470 [mole/mole]
Bath ratio	1.10235 [kg/kg]
Conc. of excess aluminum fluoride	11.50000 [%]
Conc. of dissolved alumina	2.80000 [%]
Conc. of calcium fluoride	6.00000 [%]
Heat balance:	
Superheat	5.0367 [C]
Cell energy consumption	10.2313 [kWhr/kg]
Total heat loss	516.203 [kW]
Electrical characteristics:	
Current efficiency	94.3031 [%]
Anode current density	0.658418 [A/cm*cm]
Bath resistivity	0.456250 [ohm-cm]
Cell pseudo-resistance	2.99443 [micro-ohm]
Bath voltage	0.87661 [V]
Electrolysis voltage	1.85844 [V]
Cell voltage	3.23705 [V]
Voltage to make the metal	2.03346 [V]

Steady State Solution

Cell amperage	530.0 [kA]
Anode to cathode distance	2.50000 [cm]
Operating temperature	962.298 [C]
Ledge thickness, bath level	13.14298 [cm]
Ledge thickness, metal level	7.37339 [cm]
Bath chemistry:	
Cryolite ratio	2.20470 [mole/mole]
Bath ratio	1.10235 [kg/kg]
Conc. of excess aluminum fluoride	11.50000 [%]
Conc. of dissolved alumina	2.80000 [%]
Conc. of calcium fluoride	6.00000 [%]
Heat balance:	
Superheat	5.7751 [C]
Cell energy consumption	10.0045 [kWhr/kg]
Total heat loss	477.663 [kW]
Electrical characteristics:	
Current efficiency	94.2605 [%]
Anode current density	0.658418 [A/cm*cm]
Bath resistivity	0.455863 [ohm-cm]
Cell pseudo-resistance	2.85634 [micro-ohm]
Bath voltage	0.79109 [V]
Electrolysis voltage	1.85877 [V]
Cell voltage	3.16386 [V]
Voltage to make the metal	2.03293 [V]

Table 2. Summary of all the wide cell designs produced
(T: total, B: busbar, I: internal, E: external, A: ANSYS, D/M: Dyna/Marc).

Amperage	762.5 kA	650 kA	570 kA	530 kA	530 kA
Nb. of anodes	48	36	36	36	36
Anode size	2.6m X .65m	2.6m X .86m	2.6m X .86m	2.6m X .86m	2.6m X .86m
Nb. of anode studs	4 per anode	12 per anode	12 per anode	12 per anode	12 per anode
Anode stud diameter	21.0 cm	16.0 cm	18.0 cm	18.0 cm	18.0 cm
Anode cover thickness	15 cm	25 cm	25 cm	25 cm	25 cm
Nb. of cathode blocks	24	24	24	24	24
Cathode block length	5.37 m	5.37 m	5.37 m	5.37 m	5.37 m
Type of cathode block	HC10	HC10	HC10	HC10	HC10
Collector bar size	20 cm X 12 cm	20 cm X 15 cm	20 cm X 15 cm	20 cm X 15 cm	20 cm X 15 cm
Type of side block	HC3	HC3	HC3	HC3	HC3
Side block thickness	7 cm	7 cm	7 cm	7 cm	7 cm
ASD	25 cm	25 cm	25 cm	25 cm	25 cm
Calcium silicate thickness	3.5 cm	6.0 cm	6.0 cm	6.0 cm	6.0 cm
Inside potshell size	17.02 X 5.88 m	17.02 X 5.88 m	17.02 X 5.88 m	17.02 X 5.88 m	17.02 X 5.88 m
ACD	3.0 cm	2.8 cm	2.8 cm	2.8 cm	2.5 cm
Anode current density	0.93 A/cm^2	0.81 A/cm^2	0.71 A/cm^2	0.66 A/cm^2	0.66 A/cm^2
Metal level	20 cm	20 cm	10 cm	10 cm	5 + 5 cm
Excess AlF_3	11.50%	11.50%	11.50%	11.50%	11.50%
Anode drop (A)	347 mV (T)	252 mV (T)	207 mV (I)	191 mV (I)	191 mV (I)
Cathode drop (A)	118 mV (T)	109 mV (T)	91 mV (I)	90 mV (I)	102 mV (I)
Busbar/External drop (A)	300 mV (B)	170 mV (B)	227 mV (E)	221 mV (E)	221 mV (E)
Anode panel heat loss (A)	553 kW (T)	339 kW (T)	221 kW (I)	218 kW (I)	218 kW (I)
Cathode total heat loss (A)	715 kW (T)	482 kW (T)	417 kW (I)	311 kW (I)	273 kW (I)
Operating temperature (D/M)	968.9 °C	966.5 °C	964.1 °C	961.6 °C	962.3 °C
Liquidus superheat (D/M)	10.0 °C	7.6 °C	7.5 °C	5.0 °C	5.8 °C
Bath ledge thickness (A)	6.82 cm	14.25 cm	18.36 cm	21.38 cm	19.96 cm
Metal ledge thickness (A)	1.85 cm	4.58 cm	6.88 cm	7.60 cm	5.64 cm
Current efficiency (D/M)	95.1%	94.9%	94.4%	94.3%	94.3%
Internal heat (D/M)	1328 kW	804 kW	613 kW	516 kW	478 kW
Energy consumption (D/M)	12.85 kWh/kg	11.0 kWh/kg	10.6 kWh/kg	10.2 kWh/kg	10.0 kWh/kg

3. Conclusions

The 10 kWh/kg Al barrier has been successfully reached at least on paper! Getting there required the implementation of several important design changes. The required operating conditions are also extremely challenging. Clearly a much more impressive achievement will be the successful prototyping of such a cell design operating at 10 kWh/kg Al.

4. References

32. Marc Dupuis, First attempt to break the 10 kWh/kg barrier using a wide cell design, *ALUMINIUM*, 95 (1/2), 2019, 24-29.
33. Marc Dupuis and Barry Welch, Designing cells for the future – wider and/or even higher amperage?, *ALUMINIUM*, 93 (1/2), 2017, 45-49.
34. Peter M. Entner and Marc Dupuis, Extended energy balance for Hall-Héroult electrolysis cells, *12th Australasian Aluminium Smelting Technology Conference*, Queenstown, New Zealand, 2018.
35. Peter M. Entner, *HHCellVolt AlWeb application:* http://peter-entner.com/ug/windows/hhcellvolt/toc.aspx
36. Marc Dupuis and Valdis Bojarevics, Retrofit of a 500 kA cell design into a 600 kA cell design, *ALUMINIUM*, 87(1/2), 2011, 52-55.
37. Marc Dupuis, How to limit the heat loss of anode stubs and cathode collector bars in order to reduce cell energy consumption, *Light Metals* 2019, 521-531.
38. Marc Dupuis, Presentation of a new anode stub hole design reducing the voltage drop of the connection by 50 mV, *VIII International Congress & Exhibition Non-Ferrous Metals and Minerals*, Krasnoyarsk, Russia, 13 – 16 September 2016.
39. Marc Dupuis, Breaking the 11 kWh/kg Al barrier, *ALUMINIUM*, 94 (1/2), 2018, 48-52.
40. Marc Dupuis, Very low energy consumption cell design: the cell heat balance challenge, *Light Metals*, 2018, 689-697.
41. Marc Dupuis, A new aluminium electrolysis cell busbar network concept, *Proceedings of 33rd International ICSOBA Conference*, Dubai, UAE, 29 November – 1 December 2015, Paper AL21, *Travaux* No. 44, 699-708.
42. Joseph Chaffy, Bernard Langon and Michel Leroy, Device for connection between very high intensity electrolysis cells for the production of aluminium comprising a supply circuit and an independent circuit for correcting the magnetic field, *US patent*, no 4713161, 1987.
43. Glenn Ove Linnerud and Reidar Huglen, Method for electrical connection and magnetic compensation of aluminium reduction cells and a system for same, *US patent*, no 8070921, 2011.
44. Marc Dupuis, Electrical connector system for electrolysis cell of aluminum production plant and method of using same, *Patent application*, World Intellectual Property Organization, WO/2017/020123.
45. Marc Dupuis and Hélène Côté, *Dyna/Marc 14.0 User's guide*, GeniSim, 2012.
46. Ali Al Zarouni et al., Energy and mass balance in DX+ cells during amperage increase, *31st International Conference of ICSOBA, 19th Conference Aluminium Siberia,* Krasnoyarsk, Russia, September 4 – 6, 2013, 494-498.
47. Sergey Akhmetov et al., Potline retrofit to increase productivity, *12th Australasian Aluminium Smelting Technology Conference*, Queenstown, New Zealand, 2018.
48. *SkamoAlu-Barrier-LE:* https://www.skamol.com/shop/product/skamoalu-barrier-le
49. Naixiang Feng, Aluminum electrolytic cells having heterotypic structured cathode carbon blocks, *US patent*, no 20100147678 A1, 2010.
50. René Von Kaenel, Jacques Antille and Louis Bugnion, Cathode designs and the impact on cell performance, *32nd International Conference and Exhibition of ICSOBA*, Zhengzhou, China, 12 – 15 October, 2014.